Bažant, Z.P., and Panula, L. (1978–79). "Practical prediction of time-dependent deformations of concrete." *Materials and Structures* (RILEM, Paris); Part III, "Drying creep" Vol. 11 (1978), 415–424.

Practical prediction of time-dependent deformations of concrete

Part III: Drying Creep

Z. P. BAŽANT (1), L. PANULA (2)

The practical model for predicting creep and shrinkage developed in Parts I and II is extended to creep at drying environment and constant temperature. The increase of creep due to drying is related to shrinkage. Formulas for determining material parameters from concrete strength and mix composition are presented and verified by extensive comparisons with test data from the literature.

INTRODUCTION

The prediction models for shrinkage and basic creep, developed in Parts I and II, must now be extended to cover creep in a drying environment. The expressions describing this behavior were developed in a preceding work [4] (3), and they were shown to allow good fits of test data. However, each data set was fitted individually, and no formulas that correlate the material parameters and predict them from the given concrete strength and mix composition were derived. This will be done in this part, in which data analysis of unprecedented scope (24 different mixtures) will be undertaken.

FORMULAS FOR DRYING CREEP

In [4], the creep function at simultaneous drying has been expressed as

$$J(t, t') = \frac{1}{E_0} + C_0(t, t') + C_d(t, t', t_0) - C_p(t, t', t_0), \quad (25)$$

in which $C_0(t, t')$ gives basic creep [double power law, equation (11)], C_d represents the increase of creep due to drying, C_p represents the decrease of creep after drying, t' is the age at load application, and t_0 is the age at the start of drying (both in days). The expressions for C_d and C_p, which represent only slight modifications of the expressions derived in [4], are as follows.

Creep during drying:

$$\left.\begin{aligned} C_d(t, t', t_0) &= \frac{\varphi'_d}{E_0} t'^{-m/2} k'_h \varepsilon_{sh_\infty} S_d(t, t'), \\ \varphi'_d &= \left(1 + \frac{t' - t_0}{10\tau_{sh}}\right)^{-1/2} \varphi_d. \end{aligned}\right\} \quad (26)$$

Creep after drying (predried):

$$C_p(t, t', t_0) = c_p k''_h S_p(t, t_0) C_0(t, t'). \quad (27)$$

Time shapes (similar to shrinkage):

$$\left.\begin{aligned} S_d(t, t') &= \left(1 + \frac{10\tau_{sh}}{t - t'}\right)^{-c_d n}, \\ S_p(t, t_0) &= \left(1 + \frac{100\tau_{sh}}{t - t_0}\right)^{-n}. \end{aligned}\right\} \quad (28)$$

Humidity dependence:

$$k'_h = |h_0^{1.5} - h^{1.5}|, \qquad k''_h = h_0^2 - h^2. \quad (29)$$

Here h = relative humidity of environment (constant); h_0 = initial relative humidity at which the specimen was in moisture equilibrium before time $t_0 \leqq t'$ (usually $h_0 = 0.98$ to 1.00). For a detailed discussion of these formulas *see* reference [4].

(1) Professor of Civil Engineering, Northwestern University, Evanston, Illinois 60201, U.S.A.; Active Member, RILEM.
(2) Graduate Research Assistant, Northwestern University, Evanston, Illinois 60201, U.S.A.; presently Eng., Tippetts, Abbett McCarthy and Stratton, New York.
(3) Reference numbers not listed at the end of this part are found in the preceding parts.

Equations (25)-(29) reflect various experimental properties of drying creep: (*a*) Drying that is simultaneous with creep intensifies creep (function C_d), but some time after moisture equilibrium is reached the creep is less than that of sealed wet concrete and is lower for a lower equilibrium moisture content (function C_p). (*b*) The increase of creep due to drying depends on environmental humidity and size similarly as shrinkage, as reflected in k'_h and τ_{sh}, and for very thick specimens ($\tau_{sh} \to \infty$) the drying effect must vanish. (*c*) The increase of creep due to drying is higher at a lower age (*cf.* $t'^{-m/2}$) and is higher for a concrete that shrinks more. (*d*) The later the concrete is loaded after the start of drying, the smaller the increase of creep due to drying; this is more pronounced for a thinner specimen (*cf.* φ'_d). (*e*) At the beginning of drying, and after drying as well, the creep curves have the shape of power functions. (*f*) The creep increase due to drying is delayed behind drying itself and shrinkage by approximately one log-decade, which is why equation (26) for φ'_d contains $10\tau_{sh}$ instead of τ_{sh}. (*g*) The creep decrease after drying is delayed by approximately one more log-decade, i. e., it begins long after the end of drying (reaching moisture equilibrium), which is why equation (28) for S_p contains $100\tau_{sh}$ instead of τ_{sh}. (*h*) The size-dependence conforms to the diffusion theory; indeed, all half-times (τ_{sh}, $10\tau_{sh}$, $100\tau_{sh}$) are proportional to the size-square [*see* equation (4), Part I].

The shrinkage-like function S_d causes that after the drying reaches moisture equilibrium, the slope of the creep curve in log-time decreases. From this fact, the existence of a final value of creep has often been inferred. However, according to our model, only the increase of creep due to drying reaches a final value, while the basic creep for the new equilibrium humidity probably continues without approaching a bound.

Carbonation effects have not been included in the present model. In dense, sound, uncracked concretes, the penetration of carbonation is very shallow (2 to 10 mm) and has a negligible effect unless the thickness of concrete is very small. Effects of humidity cycling are not included either. They also affect only a relatively thin surface layer, but they are undoubtedly important for thin structures, e. g., thin shells.

For derivation and detailed discussion of equations (25)-(29), the previous work [4] may be consulted. The modifications with respect to that work consist solely in using exponents $-m/2$ and $-1/2$ instead of $-m$ and -1 in equation (26), which is purely empirical.

PREDICTION OF MATERIAL PARAMETERS

By analysis of numerous test data, the following empirical formulas were derived:

$$c_p = 0.83, \qquad c_d = 2.8 - 7.5n, \tag{30}$$

for $r > 0$:

$$\left.\begin{aligned} &\varphi_d = 0.008 + 0.027u, \qquad u = \frac{1}{1+0.7r^{-1.4}}, \\ &\text{for } r \leqq 0: \ \varphi_d = 0.008, \end{aligned}\right\} \tag{31}$$

$$r = 56\,000\left(\frac{s}{a}f'_c\right)^{0.3} \times \left(\frac{g}{s}\right)^{1.3}\left(\frac{w/c}{\varepsilon_{s_\infty}}\right)^{1.5} - 0.85 \tag{32}$$

Here n = exponent given in Part II (equation 17); f'_c = 28-day cylinder strength (ksi); w/c = water-cement ratio; g/s = gravel-sand ratio; s/a = sand-aggregate ratio (all by weight); ε_{s_∞} = final shrinkage in 10^{-6} given in Part I (equation 10 *a*).

According to equation (32), an increase in strength, or in water-cement ratio, or in gravel-sand ratio, each causes an increase of the drying creep effect relative to the ultimate shrinkage, ε_{sh_∞}, and to the elastic deformation. An increase of the final shrinkage has the opposite effect. In view of equation (30), a higher ratio of the long-time creep to the short-time creep, as indicated by n (and discussed in Part II), means also a higher ratio of later to early drying creep.

COMPARISON WITH TEST DATA

The method of optimizing creep test data was the same as described for shrinkage.

Fits of 24 different comprehensive data sets available in the literature ([16], [18], [19], [36], [25], [15], [23], [20], [56], [43], [22], [58]) are exhibited in figures 19-24. All tests represent creep during drying, except Wittmann's test which gives creep after drying, and McDonald's and Kennedy's tests which give creep after resealing. Three different types of fits are shown.

The solid lines in figures 19-21 represent the fits where E_0 is determined from the reported measured static elastic modulus, using equation (12) or, if unavailable, determined by optimizing the basic creep data, φ_d is optimized, and all other parameters are calculated from the formulas [equations (30), (16-18) and (9-10)]. These fits give a picture of accuracy of the shape of the functions given in equation (26)-(29) but not of the accuracy of the magnitudes. The dashed lines in figures 19-21 represent the fits when E_0 is determined similarly as for the solid lines but φ_d is obtained from equation (31). These dashed line fits give an idea of accuracy when there is no error in the elastic modulus. Finally, figures 22-24 show fits when all material parameters, including $1/E_0$, are calculated from the preceding formulas [equations (26-32) and $1/E_0$ from equation (19)]. A picture of the accuracy of the formula for φ_d may be gained from figure 25.

With regard to Keeton's data (*fig.* 20), it must be mentioned that the last data point of each reported curve (marked as + in figure 20) was disregarded in fitting test data because it seems that the reported curves were smoothed by hand in the actual time scale, in which it is not possible to see the 'data 'trend near the end of the curve. Regarding Lambotte's data it should be noted that the curing conditions were quite unusual (exposure to drying environment at age of 24 hours).

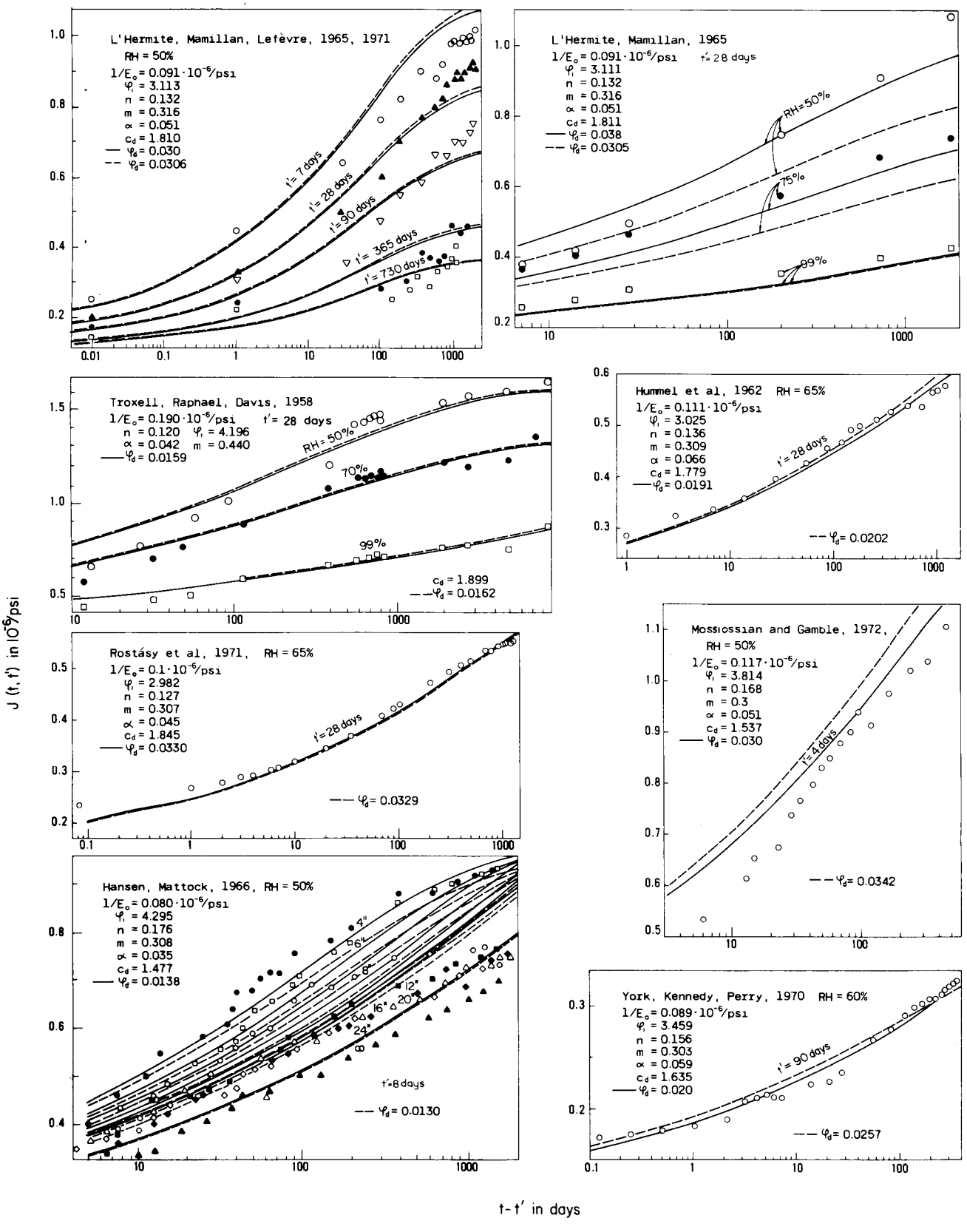

Fig. 19. — Fits of Tests for Drying Creep by L'Hermite, Mamillan and Lefèvre (1965, 1971) [16], L'Hermite and Mamillan (1965) [16], Troxell, Raphael and Davis (1958) [18], Hummel *et al.*, (1962) [19], Rostasy *et al.*, (1971) [36], Mossiossian and Gamble (1972) [25], Hansen and Mattock (1966) [15], York, Kennedy and Perry (1970) [23]. φ_d optimized – solid line, φ_d by formula – dashed line. $1/E_0$ calculated from experimental value E, if available, or optimized from basic creep data.

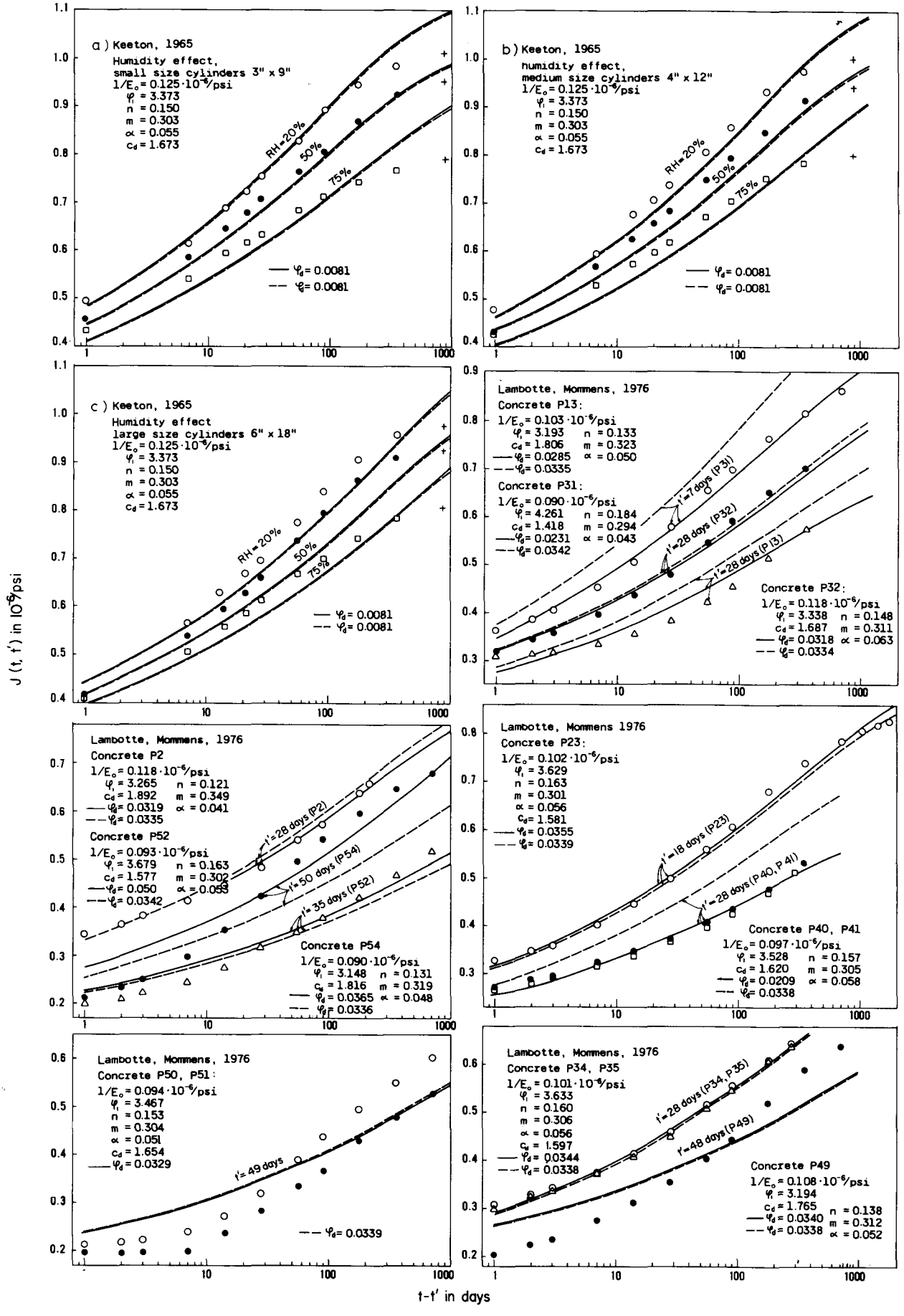

Fig. 20. – Fits of Tests for Drying Creep by Keeton (1965) [20] and Lambotte and Mommens (1976) [56]. φ_d optimized – solid line, φ_d by formula – dashed line. $1/E_0$ calculated from experimental value E, if available, or optimized from basic creep data.

The formulation has also been extended to cover the cases when the specimen is let to dry before loading and is then resealed at the time of loading, $t=t'$. In these cases φ_d and c_d should be multiplied by

$$\left.\begin{aligned}&\left[1-\left(\frac{t'-t_0}{100\,\tau_{sh}}\right)^{0.1}\right]^2\\ \text{and}\qquad&\left[1-\left(\frac{t'-t_0}{100\,\tau_{sh}}\right)^{0.1}\right],\end{aligned}\right\} \tag{33}$$

respectively, t_0 being the start of drying. Fits of such tests (McDonald's and Kennedy's) are given in figures 19, 21, 22 and 24.

A number of other test data ([24], [28], [29], [50], [57]) were analyzed. Fits of these data are not shown, however, because various important information on the tests was missing and could not be obtained.

The basic information on the test data used is summarized in Appendix III.

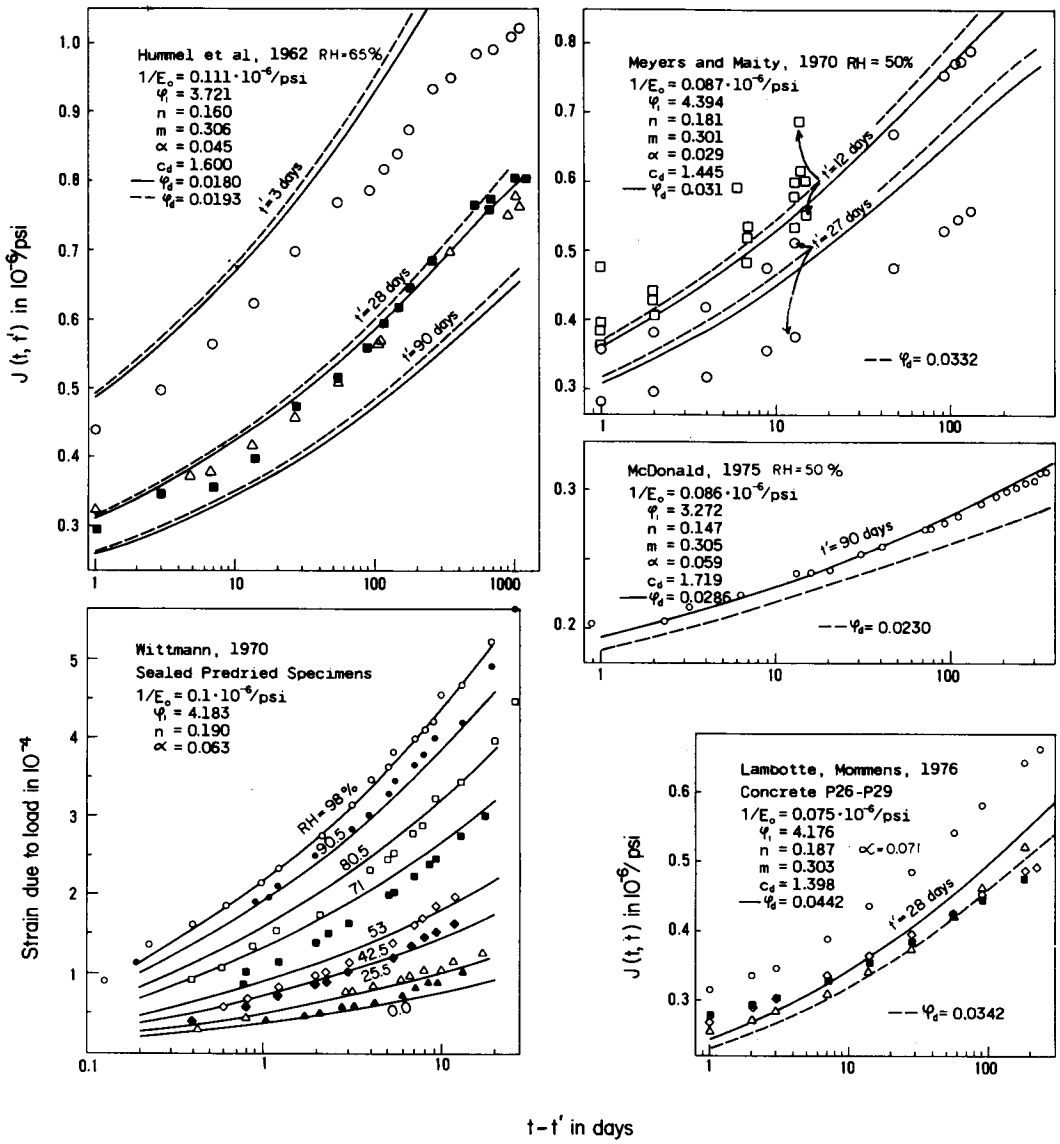

Fig. 21. — Fits of Tests for Drying Creep by Hummel *et al.*, (1962) [19], Meyers and Maity (1970) [43], Wittmann (1970) [58], McDonald (1975) [22], and Lambotte and Mommens (1976) [56]. φ_d optimized – solid line, φ_d by formula – dashed line. $1/E_0$ calculated from experimental value, E, if available, or optimized from basic creep data.

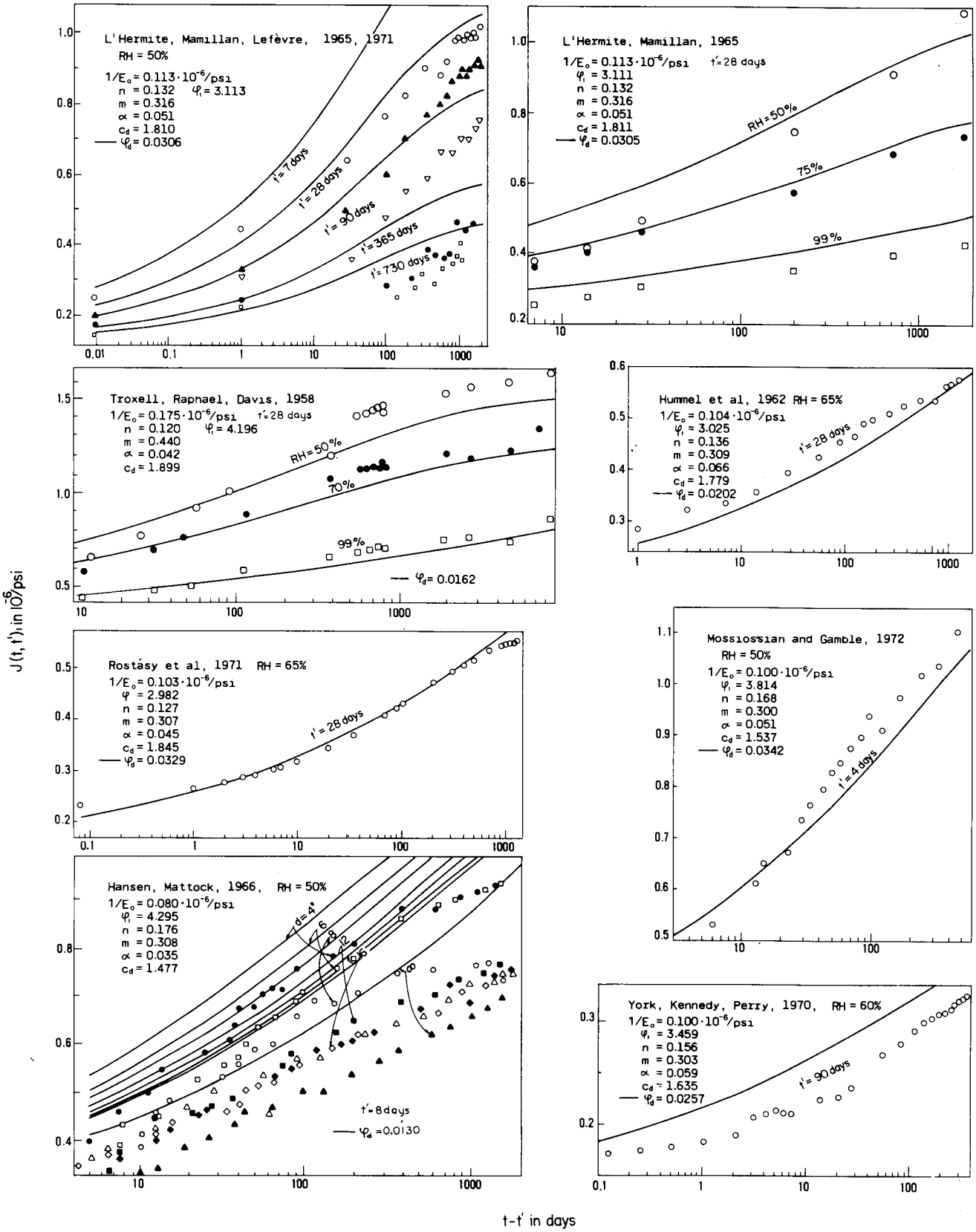

Fig. 22. — Fits of Tests for Drying Creep by L'Hermite, Mamillan and Lefèvre (1965, 1971) [16], L'Hermite and Mamillan (1965) [16], Troxell, Raphael and Davis (1958) [18], Hummel *et al.*, (1962) [19], Rostasy *et al.*, (1971) [36], Mossiossian and Gamble (1972) [25], Hansen and Mattock (1966) [15], York, Kennedy and Perry (1970) [23]. ω, and $1/E_0$ calculated by proposed formulas.

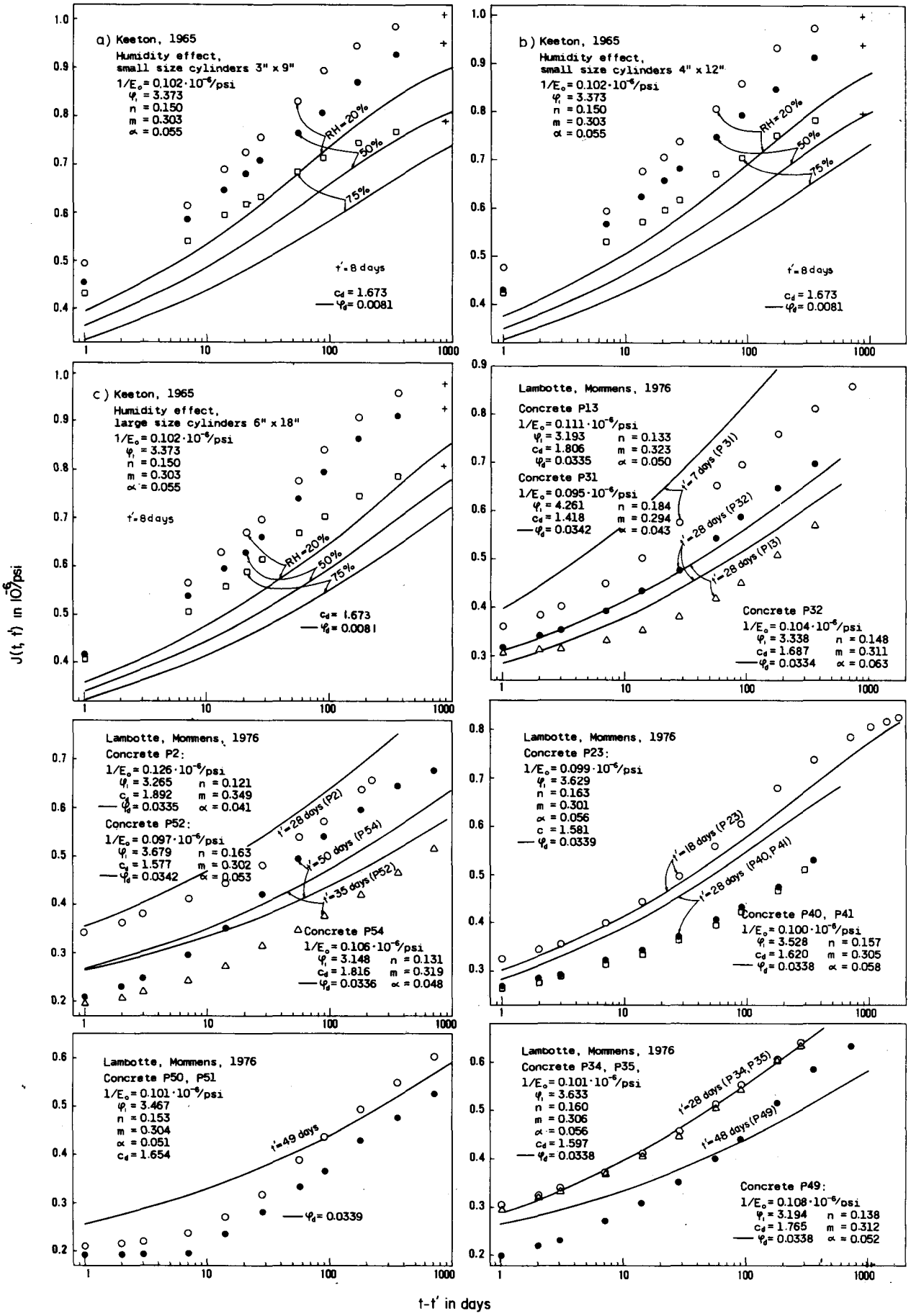

Fig. 23. — Fits of Tests for Drying Creep by Keeton (1965) [20], and Lambotte and Mommens (1976) [56]. φ_d and $1/E_0$ calculated with proposed formulas.

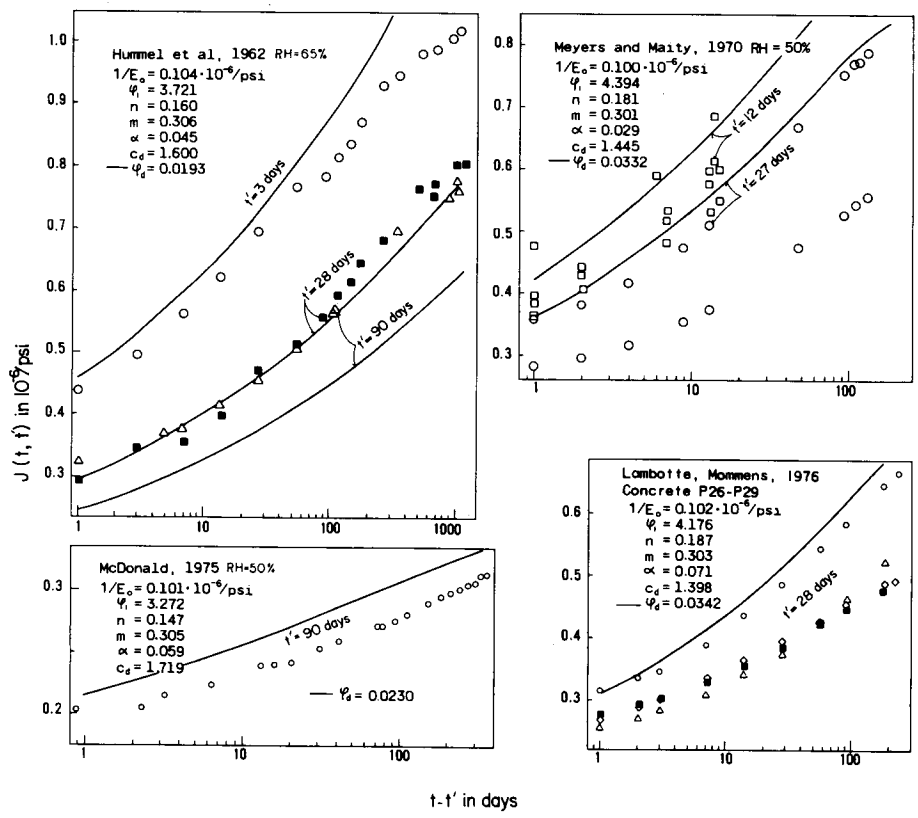

Fig. 24. — Fits of Tests for Drying Creep by Hummel *et al.*, (1962) [19], Meyers and Maity (1970) [43], McDonald (1975) [22], and Lambotte and Mommens (1976) [56]. φ_d and $1/E_0$ calculated with proposed formulas.

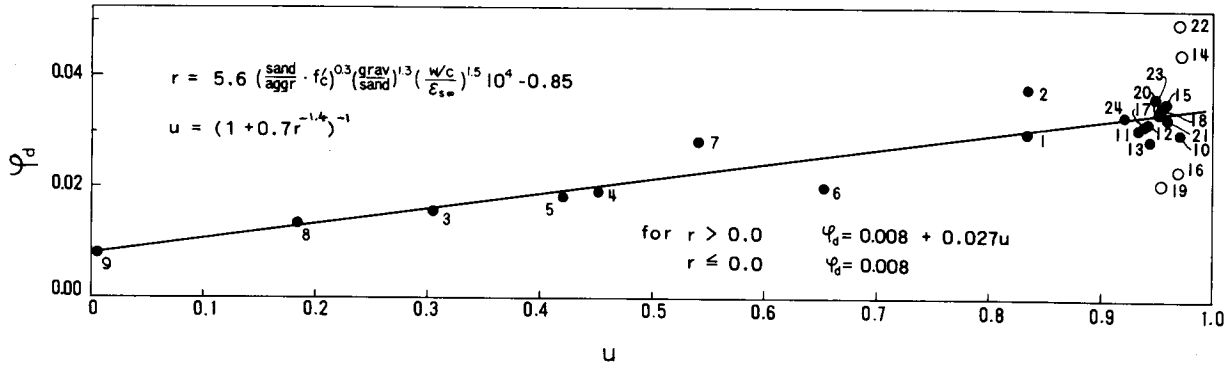

1	L'Hermite et al., RH = 50%	9	Keeton	17	Lambotte, Mommens P32
2	L'Hermite et al., var num	10	Mossiossian, Gamble	18	Lambotte, Mommens P34, P35
3	Troxell, Raphael, Davis	11	Meyers, Maity	19	Lambotte, Mommens P40, P41
4	Hummel et al., w/c = 0.38	12	Lambotte, Mommens P2	20	Lambotte, Mommens P49
5	Hummel et al., w/c = 0.55	13	Lambotte, Mommens P13	21	Lambotte, Mommens P50, P51
6	York, Kennedy, Perry	14	Lambotte, Mommens P26-P29	22	Lambotte, Mommens P52
7	McDonald	15	Lambotte, Mommens P23	23	Lambotte, Mommens P54
8	Hansen, Mattock	16	Lambotte, Mommens P31	24	Rostásy

Fig. 25. — Coefficient φ_d.

APPENDIX III

Basic Information on Test Data Used

L'Hermite, Mamillan and Lefèvre's Tests of Drying Creep (1965, 1971) [9]. – For various ages at loading. Specimens prisms 7 × 7 × 28 cm cured in water; at $t_0 = 2$ days exposed to drying at 50% relative humidity and 20°C. Portland cement 350 kg/m³. Water-cement-sand-gravel ratio 0.49 : 1 : 1.75 : 3.07. 28-day strength 370 kp/cm² (36.3 N/mm²). Aggregate Seine gravel (siliceous calcite). max. aggregate size 20 mm.

L'Hermite and Mamillan's Tests of Drying Creep (1965) [16]. – At various humidities. Specimens 7 × 7 × 28 cm cured in water 28 days, loaded at the age of 28 days and exposed to drying at relative humidities 50, 75 and 99%, temperature 20°C. Portland cement 350 kg/m³, water-cement-sand-gravel ratio 0.49 : 1 : 1.75 : 3.07. 28-day strength 370 kp/cm² (36.3 N/mm²). Aggregate Seine gravel (siliceous calcite), max. size of aggregate 20 mm.

Troxell, Raphael and Davis' Tests of Drying Creep (1958) [18]. – At various humidities. Cylinders 4 × 14 inch (102 × 356 mm) exposed at age of 28 days to drying at relative humidities 50, 75 and 99%, temperature 70°F (21°C). Cement type I, water-cement-sand-gravel ratio 0.59 : 1 : 2 : 3.67. Granite aggregate, max. aggregate size 1.5 inch (38 mm), 28-day cylinder strength 2,500 psi (17.2 N/mm²).

Rostásy *et al.*'s Tests of Drying Creep (1971) [36]. – After 7 days of curing cylinders 20 × 140 cm were exposed to drying at 65% relative humidity and 20°C temperature. Axial load applied at age of 28 days. 28-day cube strength 498 kp/cm² (48.8 N/mm²). Cement content 275 kg/m³. Water-cement-sand-gravel ratio 0.56 : 1 : 3.08 : 4. Rhine sand and Rhine gravel, max. aggregate size 30 mm.

Hansen and Mattock's Tests of Drying Creep (1966) [15]. – For various sizes of specimens. Cylinders of diameters $D = 10.2$ to 61.0 cm, and lengths 45.7, 55.9, 66.0, 86.4, 106.7, 127.0, 147.3 cm); 2 days in mold, 6 days in fog at 70°F (21°C). At the age of 8 days specimens loaded and exposed to drying at 50% relative humidity, 28 days cylinder strength 6,000 psi (41.4 N/mm²). Elgin gravel (92% calcite, 8% quartz), max. aggregate size 0.75 inch (19 mm). ASTM type III cement (362 kg/m³). Water-cement-sand-gravel ratio 0.71 : 1 : 3.3 : 2.7.

Hummel *et al.*'s Tests of Drying Creep (1962) [19]. – Mix A (*fig.* 19): After 7 days curing, cylinders 20 × 80 cm were exposed to drying at 65% relative humidity and 20°C. Axial load applied at age of 28 days. Portland cement, PZ225, 350 kg/m³, 28-day cyl. strength 414 kp/cm² (40.6 N/mm²). Water-cement-aggregate ratio 0.38 : 1 : 5.4. Mix B (*fig.* 21): Cement PZ425 (334 kg/m³). Water-cement-aggregate ratio 0.55 : 1 : 5.4. 28-day cyl. strength 435 kp/cm² (42.7 N/mm²). Specimens loaded at the ages of 3, 28 and 90 days. Rhine gravel, max. size 30 mm.

Mossiossian and Gamble's Tests for Drying Creep (1972) [25]. – Cylinders 6 × 12 inch (152 × 305 mm) were loaded and exposed to drying after 4 days of curing at 50% relative humidity and 70°F (21°C). Cement type III (418 kg/m³). Water-cement-sand-gravel ratio 0.49 : 1 : 1.35 : 2.98. Coarse aggregate: crushed limestone, max. size 1 inch (25.4 mm); 29-day cyl. strength 7,160 psi (49.4 N/mm²).

York, Kennedy and Perry's Tests of Drying Creep (1970) [23]. – After 7 days of curing cylinders 6 × 16 inch (152 × 406 mm) were exposed to drying at 60% relative humidity and 75°F (24°C). At age of 83 days specimens were sealed in copper jackets. Load applied at age of 90 days. Cement type II, 404 kg/m³. 28-day cyl. strength 6,650 psi (45.9 N/mm²). Water-cement-sand-gravel ratio 0.425 : 1 : 2.03 : 2.62. Limestone aggregate, max. size 0.75 inch (19 mm).

Keeton's Tests of Drying Creep (1965) [20]. – At various humidities and various sizes of cylinders. At age of 24 hours specimens were demolded and placed in 100% relative humidity. Load was applied and specimens were exposed to drying at 75°F (24°C) at age of 8 days. Portland cement type III (451.2 kg/m³). Water-cement-sand-gravel ratio 0.46 : 1 : 1.66 : 2.07. Max. aggregate size 0.75 inch (19 mm). Fine aggregate: Saticoy River sand, coarse aggregate: Santa Clara River gravel. 28-day cyl. strength 6,550 psi (45.2 N/mm²).

Lambotte and Mommens' Tests of Drying Creep (1976) [56]. – High strength Portland cement, except concretes P40 and P41, where early strength cement was used. Specimens cured in mold for 24 hours, then exposed to drying environment of 20°C and relative humidity 60% for all concretes, except 95% for concretes P49-P54. Specimens P2 through P41 were of size 15 × 15 × 60 cm, specimens P49 through P54 of size 10 × 10 × 40 cm.

For further data *see* table I below, in which t' is in days, f_c' is cube strength at the time of loading, in N/mm², c is cement content in kg/m³, and $w : c : s : g$ is water-cement-sand-gravel ratio.

TABLE I

Concrete	t'	f_c'	c	$w : c : s : g$
P2.....	28	32.6	270	0.611 : 1 : 2.33 : 4.74
P13.....	28	40.5	350	0.5 : 1 : 1.71 : 3.56
P26-P29.....	28	53.3 (*)	400	0.3511 : 1.06 : 3.49
P23.....	18	52.7	360	0.445 : 1 : 1.76 : 3.55
P31.....	7	47.6	400	0.575 : 1 : 1.71 : 3.04
P32.....	28	46.8	400	0.4 : 1 : 1.5 : 3.17
P34, P35.....	28	51.2	400	0.45 : 1 : 1.5 : 3.17
P40, P41.....	28	52.0	450	0.433 : 1 : 1.28 : 2.82
P49.....	48	49.8	350	0.48 : 1 : 1.85 : 3.71
P50, P51.....	49	56.6	350	0.49 : 1 : 1.85 : 3.59
P52.....	35	57.3	362	0.47 : 1 : 1.79 : 3.98
P54.....	50	45.2	350	0.52 : 1 : 1.85 : 3.71

(*) Average of four.

Wittmann's Tests of Predried Cement Paste (1970) [58]. – At various constant water content. Solid cement paste cylinders 18 × 60 mm, water-cement ratio 0.4; cured sealed for 28 days at 20°C; then dried in oven at 105°C for 2 days; then resaturated for 3 months at various constant relative humidities shown in the figure at 20°C. Then tested for creep in the same environment under stress 150 kp/cm² (14.7 N/mm²) equal 0.2 of failure load; $E = 210{,}000$ kp/cm² (20590 N/mm²) for 1 minute loading; strain at 20 minutes under load was subtracted to get the values shown.

Maity and Meyers' Tests of Drying Creep (1970) [43]. – Prisms 3.5 × 3.5 × 14 inch (89 × 89 × 356 mm), after 4 days of curing exposed to drying at 50% relative humidity and 70°F (21°C). Cement type III (253 kg/m³). Water-cement-sand-gravel ratio 0.85 : 1 : 3.81 : 3.81. Coarse aggregate: crushed limestone. 12-day cylinder strength 5,200 psi (35.9 N/mm²), cyl. 4 × 8 inch (102 × 203 mm).

McDonald's Tests of Drying Creep (1975) [22]. – After 7 days of wet curing, cylinders 6 × 16 inch (152 × 406 mm) were allowed to dry in air at 50% relative humidity and temperature 73°F (23°C). After exposing the specimens to this environment for 75 days, specimens were resealed. Load was applied at the age of 90 days. Portland cement type II (404 kg/m³). 28-day average cyl. strength 6,300 psi (43.4 N/mm²). Water-cement-sand-gravel ratio 0.425 : 1 : 2.03 : 2.62. Limestone aggregate, max. size 0.75 inch (19 mm).

REFERENCES

[56] LAMBOTTE H., MOMMENS A. – *L'Évolution du fluage du béton en fonction de sa composition, du taux de contrainte et de l'âge*, groupe de travail GT 22. Centre national de Recherches scientifiques et techniques pour l'Industrie cimentière, Bruxelles, July 1976.

[57] PIHLAJAVAARA S. E. – *A review of some of the main results of a research on the aging phenomena of concrete. Effect of moisture conditions on strength, shrinkage and creep of mature concrete.* Cement and Concrete Research, Vol. 4, 1974, pp. 761-771.

[58] WITTMANN F. – *Kriechverformung des Betons unter statischer und unter dynamischer Belastung.* Rheol. Acta., Vol. 10, 1971, pp. 422-428.

Part IV: Temperature effect on basic creep

Development of the model for basic creep in Part II is followed here by a prediction model for creep at various temperatures that are kept constant during creep. The model, which preserves the form of the double power law, reflects two opposing effects of temperature: the increase of creep rate due to heating, and the reduction of creep due to thermally accelerated hydration. Prediction of material parameters from mix composition is studied and extensive comparisons with test data indicate a good agreement.

INTRODUCTION

The double power law for basic creep, developed in Part II, will now be extended to model creep at various temperatures that are kept constant during creep. Unlike the preceding parts of this study, here we must not only model the composition influence but also decide on the proper form of the temperature effect because the model for variable temperature that we are going to investigate has not yet been proposed.

Realizing that the choice of reference temperature T_0 is subjective and largely arbitrary, we must conclude that the creep formula for any temperature (within a certain range) should have the same basic form. In particular, the form of double power law should be preserved for heated sealed concrete.

FORMULAS PROPOSED FOR TEMPERATURE EFFECT ON BASIC CREEP

Preserving its basic form, we may generalize the double power law as

$$\left.\begin{aligned} J(t,t') &= \frac{1}{E_0} + C_0(t,t'), \\ C_0(t,t') &= \frac{\varphi_T}{E_0}(t_e'^{-m} + \alpha)(t-t')^{n_T}, \end{aligned}\right\} \quad (34)$$

where

$$t_e' = \int_0^{t'} \beta_T(t'')\,dt'', \quad (35)$$

$$\varphi_T = \varphi_1(1+C_T), \qquad \beta_T = \exp\left(\frac{4\,000}{T_0} - \frac{4\,000}{T}\right). \quad (36)$$

Here C_T, n_T and β_T are functions of temperature, and t_e' represents the equivalent hydration period (or maturity) [5] (1), which is defined as the period at reference temperature T_0 needed to achieve the same degree of hydration as period t' at temperature T. Equation (36) results from assuming that the temperature effect on hydration is governed by an activation energy, Q. In equation (36), T and T_0 must be absolute temperatures. The constant 4 000°K (representing Q divided by gas constant) has been derived empirically from the data fitted in the sequel.

Following a theoretical analysis by Wittmann [58], function C_T was previously [4] suggested to also obey the activation energy concept. However, an in-depth analysis of test data revealed that this is true only for a limited range of temperatures, from about 35 to about 75°C. Beyond this range significant deviations occur, which may be due to phase changes and chemical changes, as well as simultaneous operation of several processes controlled by different activation energies. Therefore, function c_T has been identified empirically, although the basic, product form of equation (36) for φ_T, as indicated by activation energy effects, has been retained. Function c_T, which is plotted in figure 26 *a* in comparison with the activation energy dependence, has the form

$$\left.\begin{aligned} C_T &= c_T \tau_T c_0, \\ c_T &= \frac{19.4}{1+(100/(T-253.2))^{3.5}} - 1, \end{aligned}\right\} \quad (37)$$

$$\tau_T = \frac{1}{1+60/t_T'^{\,0.69}} + 0.78, \quad (38)$$

where c_0 is a composition parameter, t_T' is the age of concrete when temperature T is applied and T is absolute temperature. Note that C_T is defined not only as a function of temperature but also as a function of t_T'.

According to the activation energy model for power-type creep functions [58], exponent n_T would be a

(1) Reference numbers not listed at the end of this part are found in the preceding parts.

constant. Again, for a broader range of temperatures (−20 to 140°C) this is unacceptable. Nevertheless the form of equation (34), conforming to the activation energy model, may be retained and it suffices to take n_T as temperature-dependent. By data fitting, the following empirical function has been found:

$$n_T = B_T n, \qquad B_T = \frac{0.25}{1+(74/(T-253.2))^7} + 1. \quad (39)$$

Equation (37) is approximately valid from about −20°C to perhaps 120°C. Near the ends of the range the rise of c_T with temperature is milder (*fig. 26 a*).

Function B_T indicates that exponent n_T increases with temperature, i. e., the ratio of long-time to short-time creep increases as temperature is raised. This may be explained by the larger effect of the acceleration of aging during the early creep period.

Equations (35), (37), (38) reflect the fact that the temperature effect on creep is twofold ([60], [5]): (*a*) an increase in temperature increases the creep rate, but (*b*) it also accelerates hydration, i. e., aging. These effects, modeled by coefficients c_T, τ_T and t'_e, respectively, oppose each other. When a young concrete is heated well before it is loaded, the equivalent hydration period t'_e for the moment of load application may get sharply increased, causing a reduction of the creep increase due to heating. On the other hand, when an old concrete is heated, the change in t'_e has little effect on subsequent creep, and so a strong increase of creep with temperature takes place. Modeling of both these opposing tendencies is essential for successful fitting of test data.

The elastic modulus E is known to decrease with temperature beyond 50°C, the drop reaching about 20% at 100°C ([61], [62]). Like the double power law which gives proper age-dependence of elastic modulus, equation (34) seems to give approximately correct temperature dependence of the elastic modulus:

$$\frac{1}{E(t')} = \frac{1}{E_{stat}(t')} = J(t'+0.1, t') = \frac{1}{E_0} + \frac{\varphi_T}{E_0} 10^{-n_T}(t_e'^{-m}+\alpha). \quad (40)$$

EFFECT OF COMPOSITION ON BASIC CREEP OF HEATED CONCRETE

By fitting of test data ([59], [23], [61], [63], [64], [65], [66], [67], [68], [69], [22], [70], [71], [72]) it was verified that:

$$c_0 = \frac{1}{8}\left(\frac{w}{c}\right)^2\left(\frac{a}{c}\right)a_1, \quad (41)$$

where a_1 accounts for the cement type and is the same as in equation (18) of Part II; w/c = water-cement ratio; a/c = aggregate-cement ratio. An increase of creep rate with the water-cement ratio, as given by equation (41), is logical to expect. The increase of c_0 with the aggregate-cement ratio means that the restraining effect of aggregate on creep is stronger at lower temperatures. Equation (41) does not involve strength, but since the strength depends on w/c and a/c, the effect of strength is present indirectly.

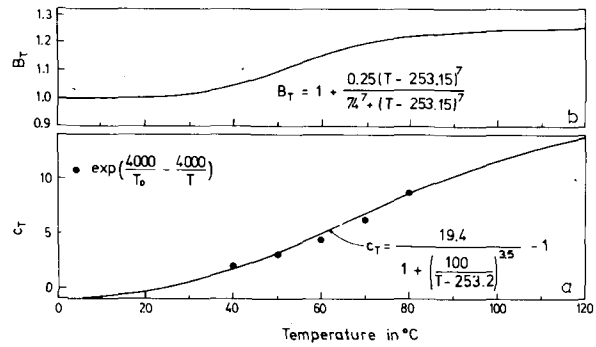

Fig. 26. — Coefficients c_T and B_T as function of temperature.

COMPARISONS WITH TEST DATA ON HEATED SEALED SPECIMENS

Fits of numerous test data shown in figures 27-34 indicate a reasonable agreement of the present model with experiments. Basic information on the test data used is given in Appendix IV.

For some data sets important information was not reported and, therefore, has had to be assumed. e. g., for England and Ross' data it has been assumed that the heat was applied at the age of 10 days, simultaneously with load application (i. e., no heat stabilization period before the test). Also, the initial "elastic" strains at elevated temperatures have been assumed using proportionality to the values of Maréchal. For the tests of Silveira and Florentino, it has been assumed that the heat was applied three days before loading.

For Nasser and Neville's data ([68], [69]), the sand-gravel ratio was not available, and so exponent n has been assumed. The initial elastic strains have had to be assumed also (0.2×10^{-6}/psi). Papers [68] and [69] mentioned that E was not a function of temperature; therefore, the value of $1/E_0$ has been found by optimization. The E-modulus was reported to increase by 22% from $t'=14$ days to $t'=365$ days, and the value of $J(t'+0.001, t')$ has been assumed to change in proportion. Moreover, these data indicate, independently of curing temperature, a 22% increase of elastic modulus upon heating, which conflicts with references [61] and [62]. The deviations from test data in figures 28 and 32 must be judged in the light of the preceding remarks.

When unspecified, the unit weight of concrete has been assumed as 2,400 kg/m^3.

It is interesting to compare $J(90+365, 90)$ for the data of Silveira and Florentino [67], McDonald [22] and Kennedy [23]. At room temperature, the values are 0.425, 0.285, 0.285 (all in 10^{-6}/psi), and at elevated temperatures tested (45, 65.6 and 65.6°C respectively), the values are 0.748, 0.400 and 0.445. This is a considerable scatter in view of the fact that the mix parameters and test conditions were quite similar (*see* Appendix IV).

For temperatures beyond 95°C, the present model gives only very crude estimates. Even though all

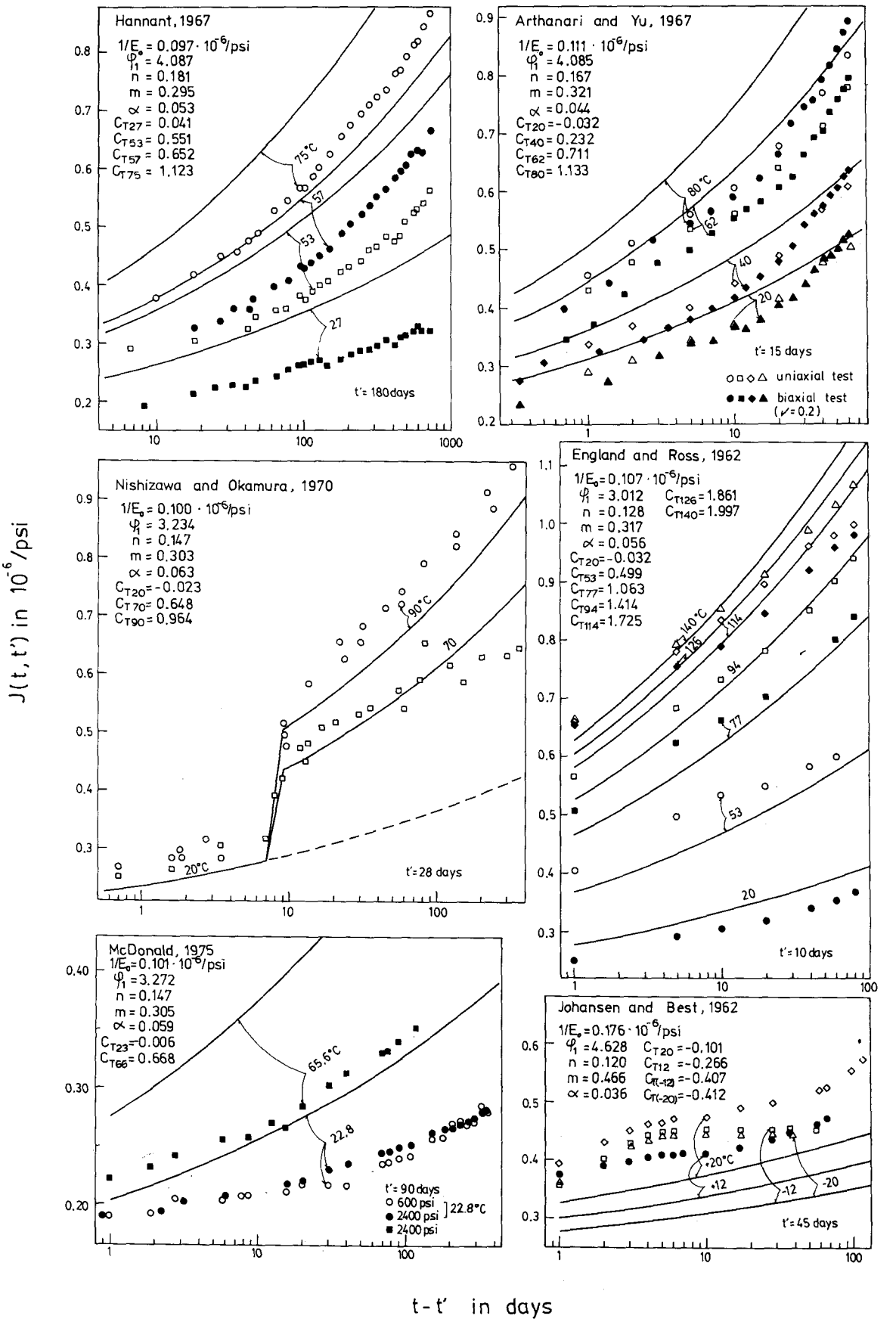

Fig. 27. – Fits of Tests of Temperature Effect on Creep by Hannant (1967) [61], Arthanari and Yu (1967) [63], Nishizawa and Okamura (1970) [64], England and Ross (1962) [65], McDonald (1975) [22] and Johansen and Best (1962) [66]. C_T optimized – solid line; subscript number refers to corresponding temperature. C_T with formula – dashed line. $1/E_0$ calculated from experimental E_{28} or optimized from basic creep data.

specimens considered here were sealed, moisture may have moved out of concrete and collected under a bulged jacket. Also, rapid redistribution of moisture within the heated specimen may have had considerable effect on creep. In particular, the present model does not describe the decrease in creep rate (i. e., in C_T) that is sometimes observed upon passing 100°C; see the curves near 100°C in figure 28 for Nasser and Neville's data, and the reversed order of temperatures for the curves near 100°C in figure 27 for England and Ross's data.

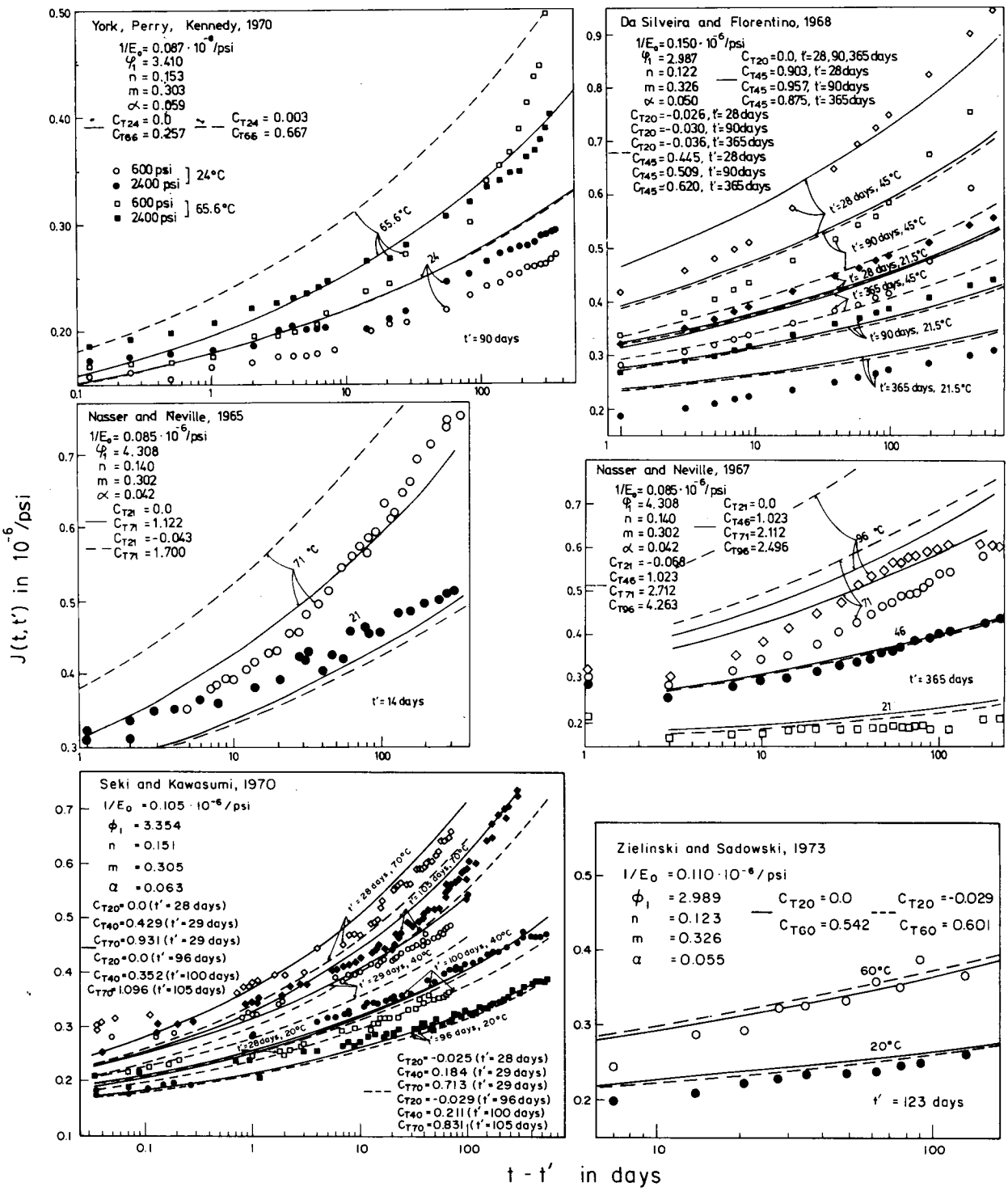

Fig. 28. – Fits of Tests of Temperature Effect on Creep by York, Kennedy and Perry (1970) [23], Da Silveira and Florentino (1968) [67], Nasser and Neville (1965) [68], Nasser and Neville (1967) [69], Seki and Kawasumi (1970) [70] and Sielinski and Sadowski (1973) [71]. C_T optimized – solid line, C_T with formula – dashed line. $1/E_0$ optimized from basic creep data.

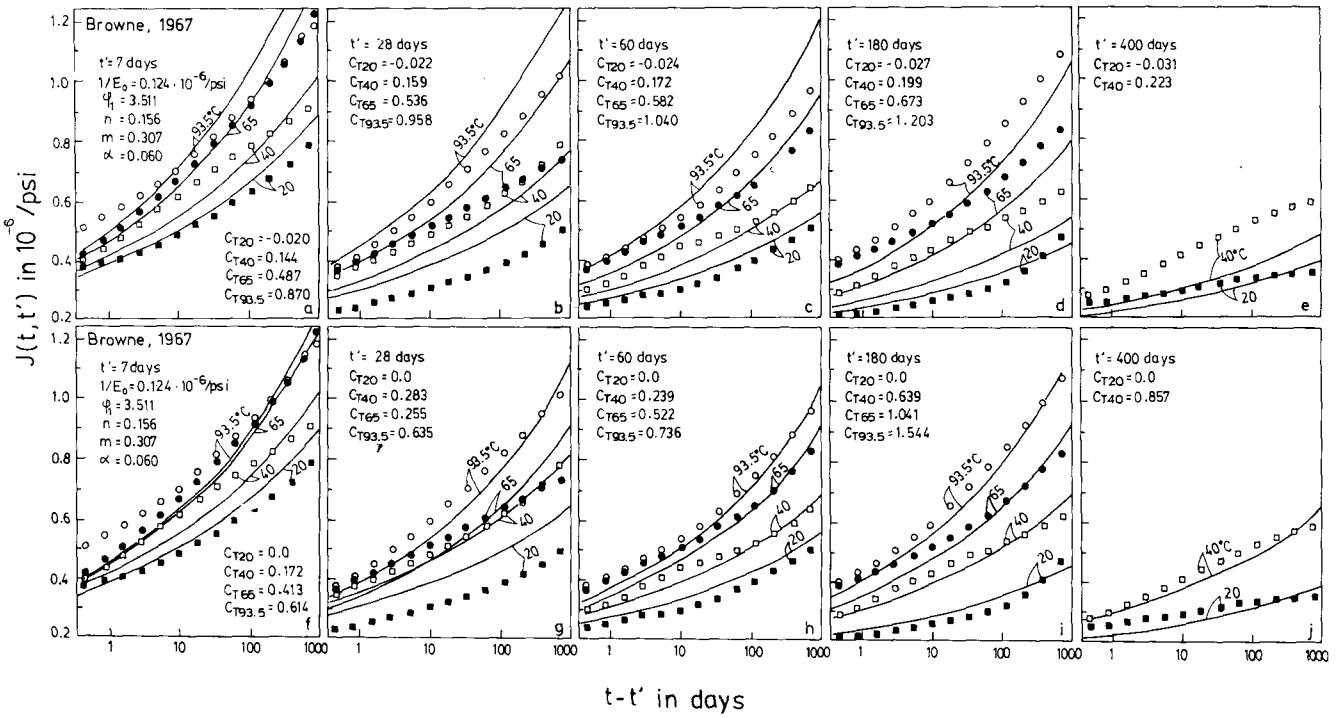

Fig. 29. – Fits of Tests of Temperature Effect on Creep by Browne (1967) [59]. C_T optimized – solid line in figure *f-j*. C_T with formula – solid line in figure *a-e*. $1/E_0$ optimized from basic creep data. Experimental datas are smoothed mean values.

APPENDIX IV

Basic Information on Test Data Used

Hannant's Tests of Temperature Effect on Creep (1967) [61]. – Cylinders 4 $\frac{1}{8} \times 12$ inch (105 × 305 mm), cured for 24 hours in molds under wet rags, then 5 months under water at 20°C, and then one month sealed in copper. Heating rates about 10°C/hr. For temperature stabilization all specimens were heated for 24 hours before loading. Stress 2,000 psi (13.8 N/mm²). Water-cement-sand-gravel ratio 0.47 : 1 : 1.845 : 2.655. Sulphate resisting Portland cement with Plastocrete plasticizer. Coarse aggregate limestone max. size 3/8 inch (10 mm). 28-day cube strength 9,350 psi (64.5 N/mm²).

Nishizawa and Okamura's Tests of Temperature Effect on Creep (1970) [64]. – Specimens 15 × 15 × 55 cm, sealed in copper, prestressed to compressive stress 120 kg/cm² (11.8 N/mm²) at the age of 28 days. After 7 days of loading at 20°C, specimens exposed to temperature of 70 or 90°C. Water-cement-ratio 0.40, cement content 377 kg/m³, sand percentage 36.5%. (In calculations water-cement-sand-gravel ratio 0.40 : 1 : 1.85 : 3.22 was used.) Max. size of coarse aggregate = 25 mm, normal cement. Cylinder strength 459 kg/cm² (45 N/mm²).

McDonald's Tests of Temperature Effect on Creep (1975) [22]. – Cylinders 6 × 16 inch (152 × 406 mm) demolded after 24 hours, coated with epoxy and returned to fog room. After 24 hours another coat of epoxy, and sealed in copper. At age of 83 days, specimens recoated with epoxy, sealed in neoprene, and placed to environment of test temperature, loaded at age of 90 days. Water-cement-sand-gravel ratio 0.425 : 1 : 2.03 : 2.62. Type II portland cement (404 kg/m³). Limestone aggregate, max. size 3/4 inch (19 mm). 28-day average cyl. strength 6,300 psi (43.4 N/mm²).

Arthanari and Yu's Tests of Temperature Effect on Creep (1967) [63]. – Slabs 12 × 12 × 4 inch (305 × 305 × 102 mm), cured under wet hessian for 7 days. For tests under mass-concrete conditions sealed by epoxy resin and two coats of plastic emulsion paint. Loaded at age of 15 days, stress 1,000 psi (6.9 N/mm²). Heating began 1 day before loading. Water-cement-sand-gravel ratio 0.564 : 1 : 1.125 : 2.625. Thames river gravel of size 3/16-3/8 inch (4.76-9.5 mm), ordinary portland cement. 28-day average cube strength 6,000 psi (41.4 N/mm²).

England and Ross' Tests of Temperature Effect on Creep (1962) [65]. – Cylinders 4.5 × 12 inch (114 × 305 mm), demolded at age of 1 day, placed under water for additional 3 days, after which stored at 17°C and 90% R.H. until tested at age of 10 days in a sealed state. The seal was a polyester resin, with fibre glass reinforcement. Water-cement-sand-gravel ratio 0.45 : 1 : 2 : 4. Compressive strength of 4 inch (102 mm) cubes at age of 14 days = 5,500 psi (37.9 N/mm²). Elastic modulus 5×10^6 lb/in² (34,480 N/mm²).

Johansen and Best's Tests of Temperature Effect on Creep (1962) [66]. – Cylinders 10 × 30 cm and 15 × 30 cm cast in steel molds and remolded at age of 1 day, then stored at 100% rel. humidity and 20°C. At age of 42 days, specimens were sealed and moved to test environment. At the end of 3 days stabilization period specimens were loaded at their respective temperatures to 30% of their ultimate strength in compression as measured at 20°C. Water-cement-sand-gravel ratio 0.7 : 1 : 3.5 : 3.5. Normal portland cement. Max. size of aggregate 3/8 inch (9.5 mm). Average compressive strength 179 kp/cm² (17.6 N/mm²) at the age of 42 days on cylinders 15 × 30 cm.

York, Kennedy and Perry's Tests for Temperature Effect on Creep (1970) [23]. – Cylinders 6 × 16 inch (152 × 406 mm), removed from molds 24 hours after casting. Then epoxy coat applied and specimens stored in fog room. Next, 48 hours after casting, specimens sealed in copper and placed in test environment at 73.4°F (23°C). At age of 83 days specimens sealed in neoprene jacket, and exposed to test temperature. Loaded at age of 90 days. Water-cement-sand-gravel ratio 0.425 : 1 : 2.03 : 2.62. Cement type II (404 kg/m³). Limestone aggregate, max. size 3/4 inch (19 mm); 28-day cyl. strength 6,560 psi (45.2 N/mm²).

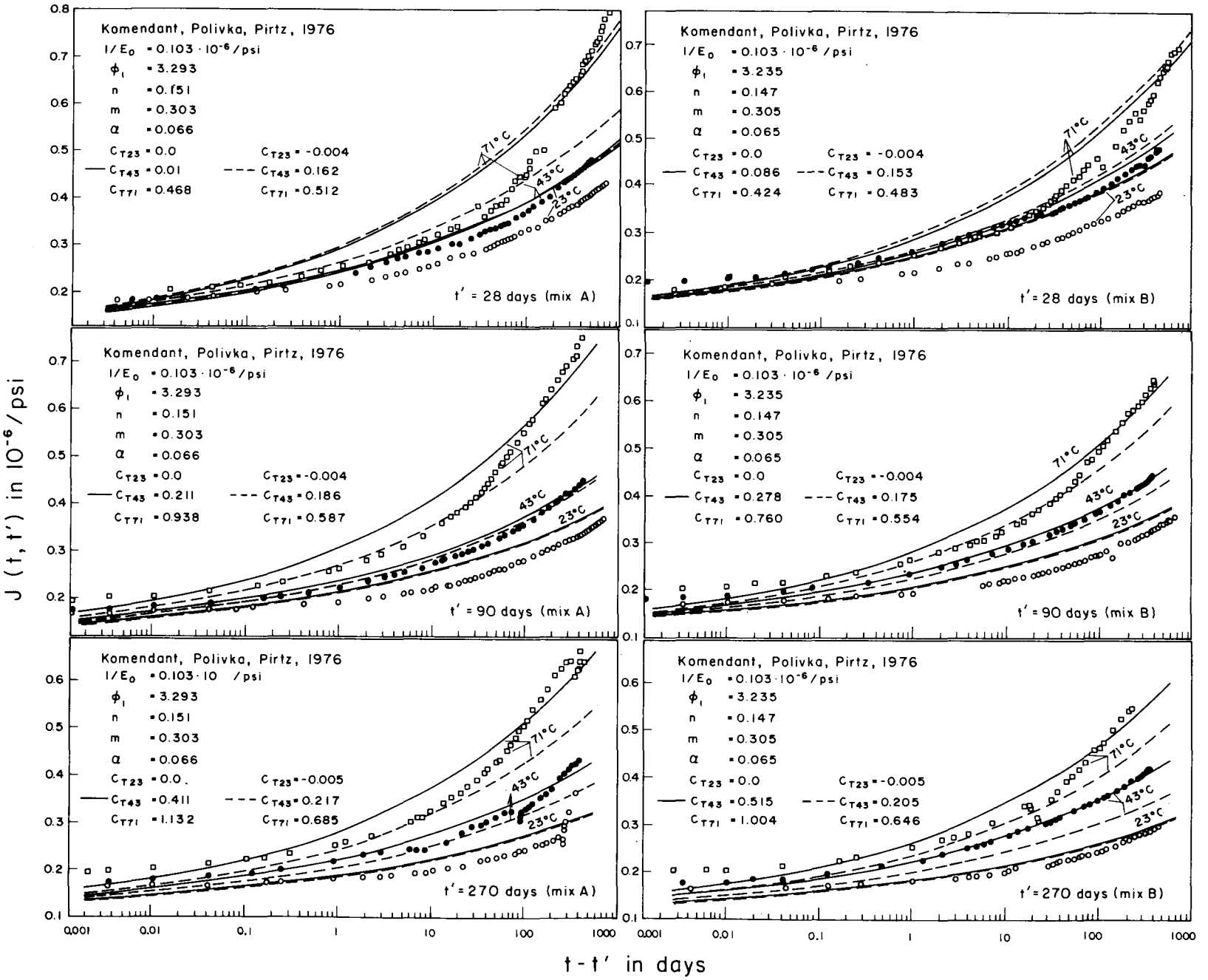

Fig. 30. – Fits of Tests of Temperature Effect on Creep by Komendant, Polivka and Pirtz (1976) [72]. C_T optimized – solid line, C_T with formula – dashed line. $1/E_0$ optimized from basic creep data.

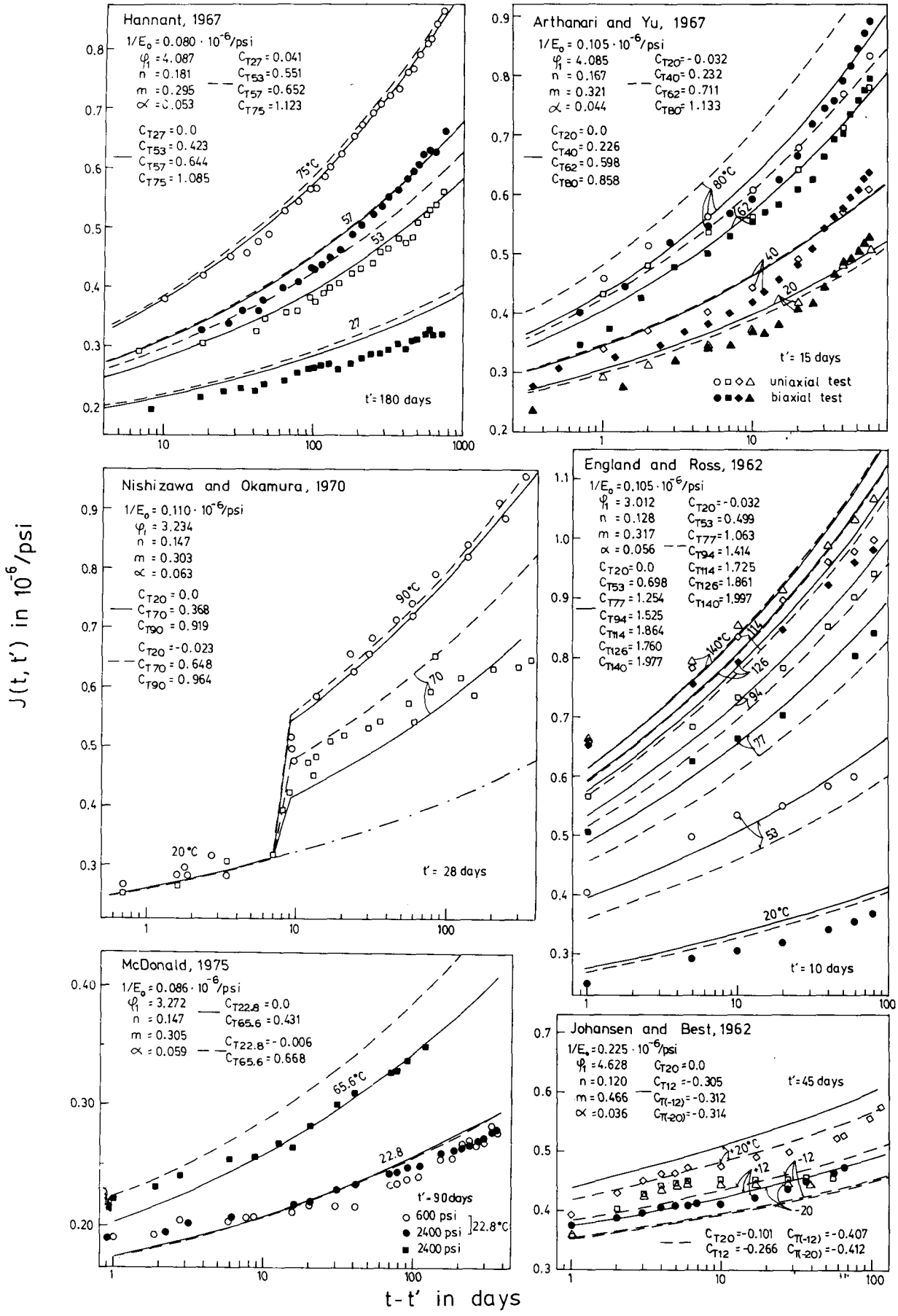

Fig. 31. – Fits of Tests of Temperature Effect on Creep by Hannant (1967) [61], Arthanari and Yu (1967) [63], Nishizawa and Okamura (1970) [64], England and Ross (1962) [65], McDonald (1975) [22] and Johansen and Best (1962) [66]. C_T and $1/E_0$ both calculated with formula.

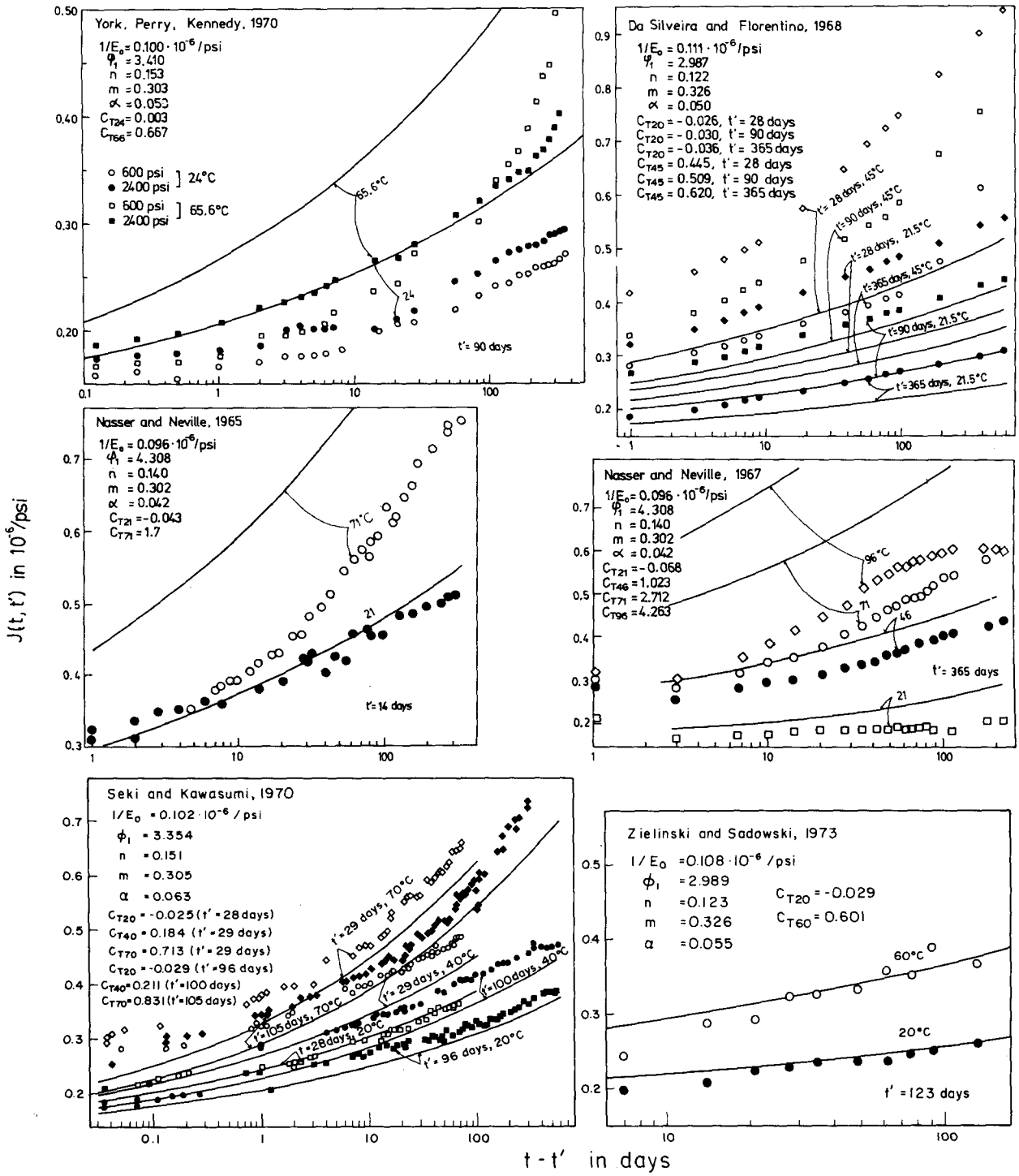

Fig. 32. – Fits of Tests of Temperature Effect on Creep by York, Kennedy and Perry (1970) [23], Da Silveira and Florentino (1968) [67], Nasser and Neville (1965) [68], Nasser and Neville (1967) [69], Seki and Kawasumi (1970) [70], Zielinski and Sadowski (1973) [71]. C_T and $1/E_0$ both calculated with formula.

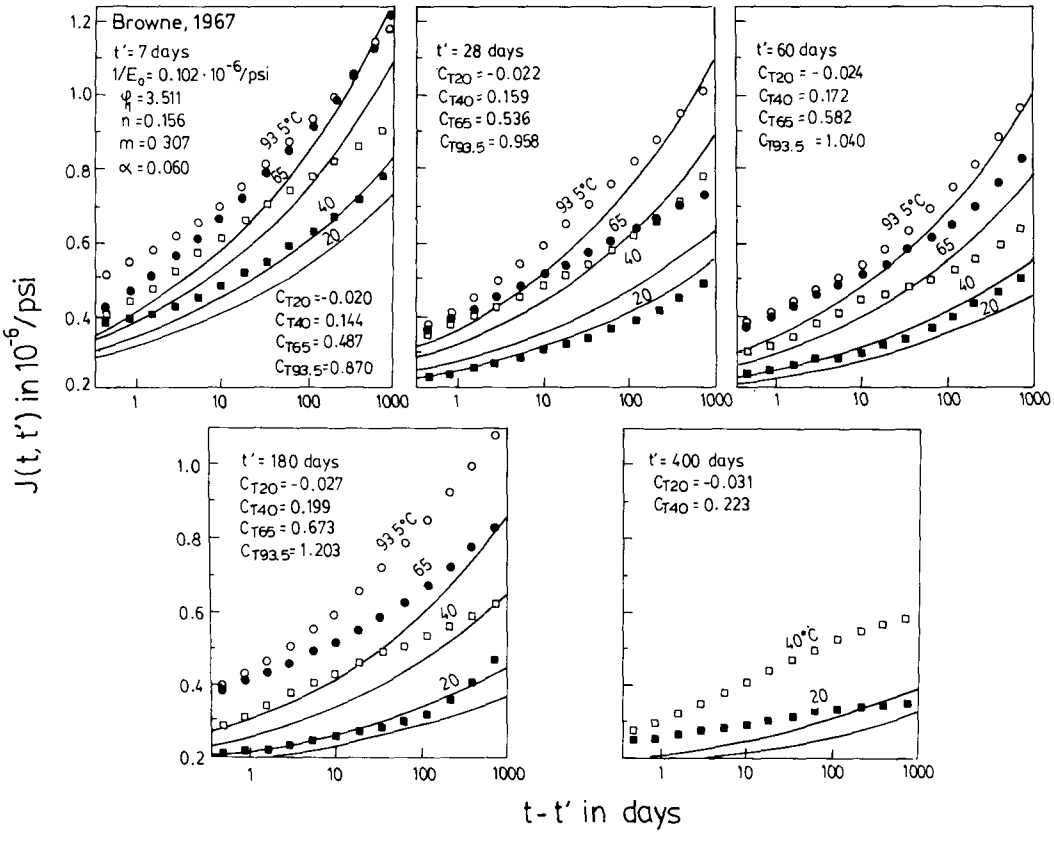

Fig. 33. – Fits of Tests of Temperature Effect on Creep by Browne (1967) [59]. C_T and $1/E_0$ both calculated with formula. Experimental datas are smoothed mean values.

Da Silveira and Florentino's Tests of Temperature Effect on Creep (1968) [67]. – Prisms 20 × 20 × 60 cm, in copper jackets. Heat is assumed to be applied 3 days before loading. Water-cement-sand-gravel ratio 0.5 : 1 : 2.35 : 3.84. Granite aggregate, modified portland cement, similar to ASTM type II. Cement content 314.6 kg/m³, 8-day cube strength 297 kp/cm² (29.1 N/mm²).

Nasser and Neville's Tests of Temperature Effect on Creep (1965) [68]. – Cylinders 3 × 9 $\frac{1}{4}$ inch (76 × 235 mm), sealed in polypropylene jackets, stored from 24 hours onwards in a water bath at the desired temperature and loaded at age of 14 days. Water-cement ratio 0.6 and aggregate-cement ratio 7.15. Max. size of aggregate 3/4 inch (19 mm). Aggregate was a mixture of dolomite and hornblende. Cement type III (320 kg/m³). Strength 5,660 psi (39 N/mm²) at 14 days measured on cylinders 3 × 9 $\frac{1}{4}$ inch (76 × 235 mm). Stress/strength ratio 0.35.

Nasser and Neville's Tests of Temperature Effect on Creep (1967) [69]. – Cylinders 3 × 9 $\frac{1}{4}$ inch (76 × 235 mm), stored in water at 70°F (21°C) up to 1 week prior to application of load. Concrete 1 : 7.15 mix; water-cement ratio of 0.6. Max. size of dolomite and hornblende aggregate was 3/4 inch (19 mm), cement type III (320 kg/m³). Specimens loaded at age of 1 year and remained under water while loaded. Mean strength at the time of load application (determined on specimens of same size) = 7,250 psi (50 N/mm²).

Browne's Tests of Temperature Effect on Creep (1967) [59]. – Cylinders 6 × 12 inch (152 × 305 mm), sealed at casting in 1/16 inch (1.6 mm) polypropylene jackets, cured at room temperature. Heat applied 1 day before loading. Water-cement–sand–gravel ratio 0.42 : 1 : 1.45 : 2.95. Ordinary portland cement, crushed foraminiferal limestone, max. size 1.5 inch (38 mm). Average 6 inch (15.2 cm) cube strength = 7,250 psi (50 N/mm²).

Zielinski and Sadowski's Tests of Temperature Effect on Creep (1973) [71]. – Cylinders 160 × 480 mm within the first 70 days stored in atmosphere 100% relative humidity and temperature 20-23°C, then sealed with rubber coat. Specimens were heated at the age of 120 days and loaded three days later. Water-cement-aggregate ratio 0.456 : 1 : 4.154. Sand/cement-gravel/cement ratio assumed to be 1.9 : 2.254. Cement ordinary Portland Cement type I, 450 kg/m³, aggregate crushed basalt and river sand, max. size 20 mm. 120 day compressive cylinder (160 × 160 mm) strength 430 kg/cm².

Seki and Kawasumi's Tests of Temperature Effect on Creep (1970) [70]. – Cylinders 150 × 600 mm were cast into 0.2 mm copper jackets. Specimens loaded at room temperature (20°C) at the age of 28 and 96 days. The temperature 40°C was applied at the age of 28 and 97 days and loaded at the age of 29 and 100 days. The temperature 70°C was applied at the age of 27 and 104 days and specimens loaded when they were 29 and 105 days old. Water-cement-sand-aggregate ratio 0.4 : 1 : 1.761 : 3.834. Normal Portland cement 343 kg/m³, fine aggregate Fuji-Gawa river sand, coarse aggregate from the river Ara-Kawa. 28-day cylinder strength 445 kp/cm².

Komendant, Polivka and Pirtz's Tests of Temperature Effect on Creep (1976) [72]. – Cylinders 6 × 16 inch (152 × 406 mm) sealed with butyl rubber against moisture loss and cured at 73°F (23°C) until five days prior to the age of loading. The specimens were then heated to test temperatures 110 and 160°F (43 and 71°C) at a rate of 24°F/day (13.3°C/day) and remained for the duration of the creep test. Specimens were loaded at the age of 28, 90 and 270 days. Cement, Medusa type II. Mix A: water-cement-sand-gravel ratio 0.381 : 1 : 1.734 : 2.605; 28-day cylinder strength 6,590 psi (45.4 N/mm²). Cement 706 lbs/cy (419 kg/m³). Max size of aggregate 1.5 inch.

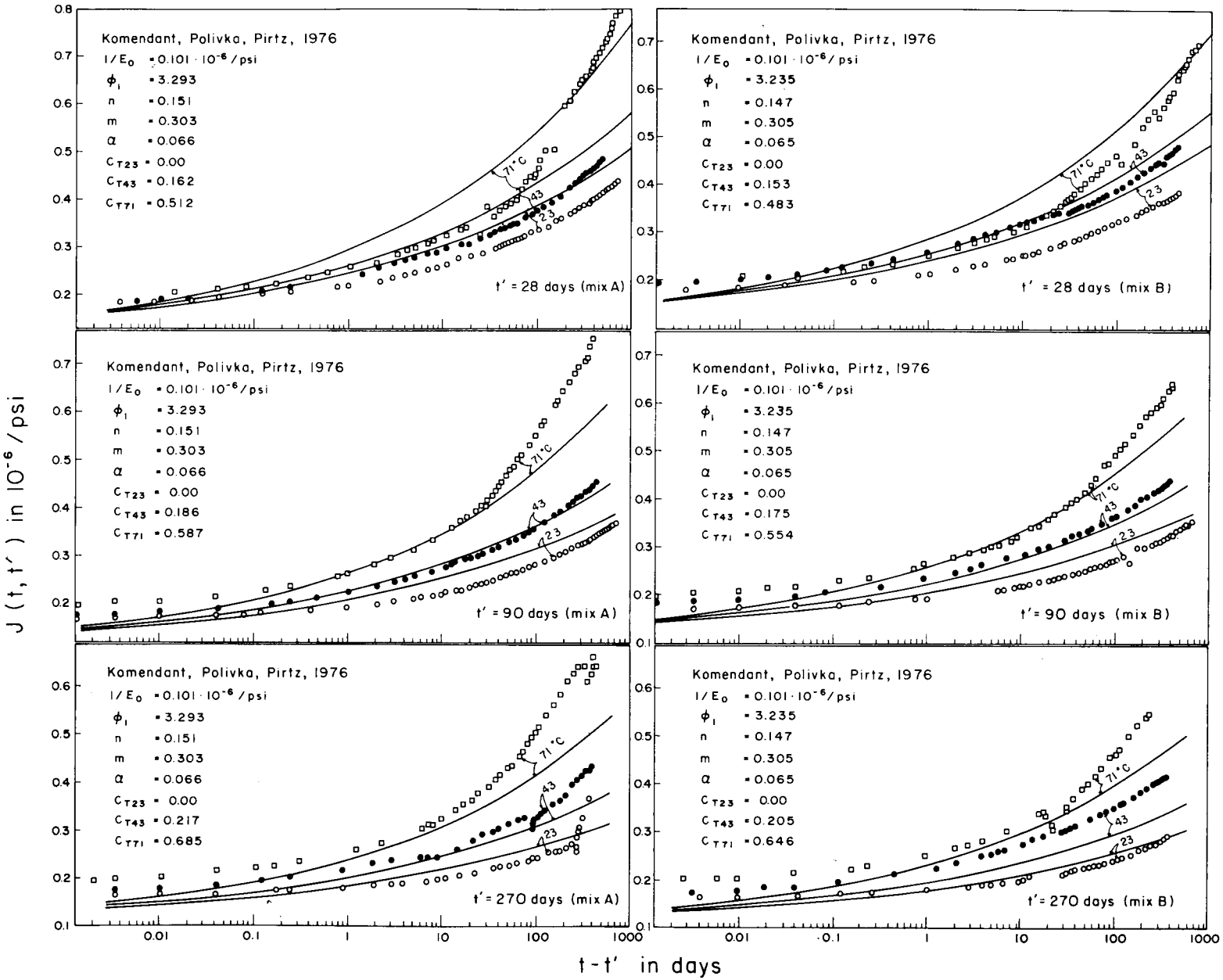

Fig. 34. – Fits of Tests of Temperature Effect on Creep by Komendant, Polivka and Pirtz (1976) [72]. C_T and $1/E_0$ both calculated with formula.

REFERENCES

[59] BROWNE R. D. – *Properties of concrete in reactor vessels.* Proceedings, Conference on Prestressed Concrete Pressure Vessels, Institution of Civil Engineers, London, England, group C, paper 13, 1967, pp. 11-31.

[60] BAŻANT Z. P., WU S. T. – *Thermoviscoelasticity of aging concrete.* Journal of the Engineering Mechanics Division, ASCE, Vol. 100, No. EM3, Proc. Paper 10621, June, 1974, pp. 575-597.

[61] HANNANT D. J. – *Strain behaviour of concrete up to 95°C under compressive stresses.* Group C, paper 17. Conference on Prestressed Concrete Pressure Vessels, Institution of Civil Engineers, London 1967, pp. 57-71.

[62] MARÉCHAL J. C. – *Variations in the modulus of elasticity and Poisson's ratio with temperature.* Paper SP34-27. Concrete for nuclear reactors, Vol. I, ACI Special Publication SP-34. American Concrete Institute, Detroit, Michigan, 1972, pp. 495-503.

[63] ARTHANARI S., YU C. W. – *Creep of concrete under uniaxial and biaxial stresses at elevated temperatures.* Magazine of Concrete Research, Vol. 19, No. 60, September 1967, pp. 149-155.

[64] NISHIZAWA N., OKAMURA H. – *Strength and inelastic properties of concrete at elevated temperature.* Paper SP34-22. Concrete for nuclear reactors, Vol. I, ACI Special Publication SP-34 American Concrete Institute, Detroit, Michigan 1972, pp. 407-421.

[65] ENGLAND G. L., ROSS A. D. – *Reinforced concrete under thermal* gradients. Magazine of Concrete Research, Vol. 14, No. 40, March 1962, pp. 5-12.

[66] JOHANSEN R, BEST C. H. – *Creep of concrete with and without ice in the system.* Bulletin RILEM, No. 16, September 1962, pp. 47-57.

[67] DA SILVEIRA A., FLORENTINO C. A. – *Influence of temperature on the creep of mass concrete.* Paper SP25-7. Temperature and concrete. ACI Publication SP-25. American Concrete Institute, Detroit, Michigan, 1971, pp. 173-189.

[68] NASSER K. W., NEVILLE A. M. – *Creep of concrete at elevated temperatures,* Journal of the American Concrete Institute, Vol. 62, December 1965, pp. 1567-1579.

[69] NASSER K. W., NEVILLE A. M. – *Creep of old concrete at normal and elevated temperatures,* Journal of the American Concrete Institute, Vol. 64, February 1967, pp. 97-103.

[70] SEKI S., KAWASUMI M. – *Creep of concrete at elevated temperatures.* Paper SP34-32. Concrete for nuclear reactors, Vol. I, ACI Special Publication SP-34, American Concrete Institute, Detroit, Michigan, 1972, pp. 591-638.

[71] ZIELINSKI J. L., SADOWSKI A. – *The influence of moisture content on the creep of concrete at elevated temperatures,* 2nd International Conference on Structural Mechanics in Reactor Technology, 1973, paper H6/3, pp. 1-8.

[72] KOMENDANT G. J., POLIVKA M., PIRTZ D. – *Study of concrete properties for prestressed concrete reactor vessels,* Final report-part II, *Creep and strength characteristics of concrete at elevated temperatures,* Report No. UC SESM 76-3, Structures and Materials Research, Department of Civil Engineering, Report to General Atomic Company, San Diego, California Berkeley, California, April 1976.

RÉSUMÉ

Un modèle de prévision pratique des déformations du béton en fonction du temps. III. Fluage en séchage. – *Le modèle pratique de détermination du fluage et du retrait exposé dans les parties I et II de ce mémoire est à présent appliqué au fluage en ambiance sèche et à température constante. L'augmentation du fluage due au séchage est reliée au retrait. On donne les formules pour déterminer les paramètres des matériaux à partir de la résistance du béton et de la composition du mélange, et on les vérifie par des comparaisons nombreuses avec les résultats d'essai publiés.*

IV. Influence de la température sur le fluage de base. – *Le développement d'un modèle pour le fluage de base qui est l'objet de la deuxième partie de ce mémoire est suivi ici par un modèle de détermination du fluage à différentes températures maintenues constantes durant le phénomène. Ce modèle qui préserve la loi de double puissance traduit deux effets contraires de la température : l'augmentation de la vitesse du fluage due à la chaleur et la diminution du fluage due à l'accélération de l'hydratation par la chaleur. L'étude comprend la détermination des paramètres des matériaux à partir de la composition du mélange et de nombreuses comparaisons avec les résultats d'essai indiquent une bonne concordance.*

To be continued by Parts V and VI.